Electronic Supplementary Material (ESI) for Nanoscale.

High throughput near infrared screening discovers DNA-templated silver clusters with peak fluorescence beyond 950 nm

Steven M. Swasey[1], Stacy M. Copp[2], Hunter C. Nicholson[3], Alexander Gorovits[4], Petko Bogdanov[4] and Elisabeth G. Gwinn[2]

[1]*Department of Chemistry and Biochemistry, UCSB, Santa Barbara California, 93106, USA*
[2]*Center for Integrated Nanotechnologies, Los Alamos National Laboratories, Los Alamos, NM 87545, USA*
[3]*Department Physics, UCSB, Santa Barbara California, 93106, USA*
[4]*Department of Computer Science, University at Albany, SUNY, Albany NY 12222*

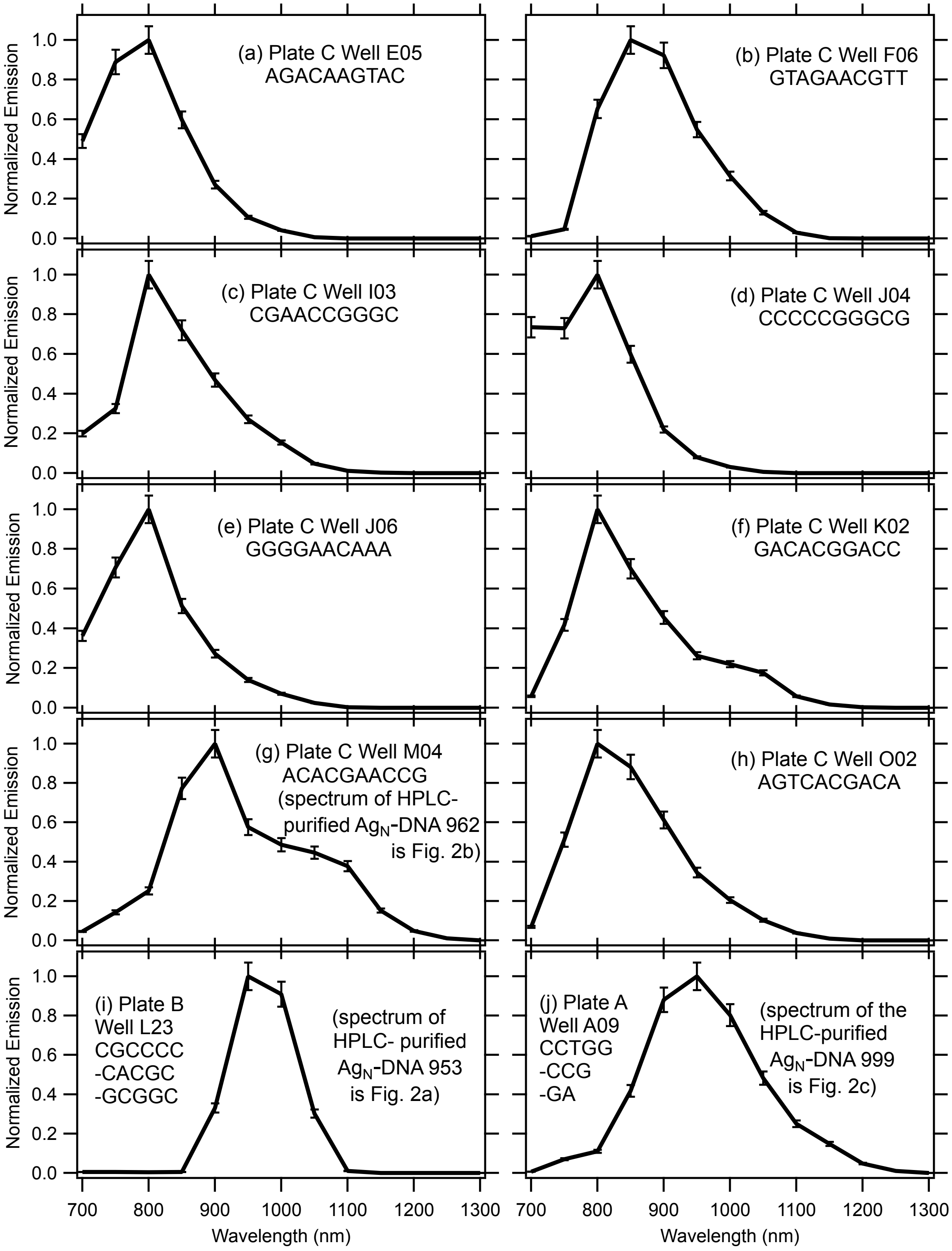

Figure S1. NIR emission spectra for unpurified Ag_N-DNA solutions of the ten candidate templates selected for synthesis scale-up and attempted HPLC purification. Microplate (A, B or C), well location and template sequence are identified on the plots. Fluorescence was excited in the UV, as described in the main text. Error bars are instrumental uncertainty. Data are corrected for the spectral responsivity of the InGaAs detector in the NIR fluorescence microplate reader. HPLC purification narrows and shifts the spectra in Fig. 2 of the main text relative to the unpurified spectra in (g), (i) and (j).

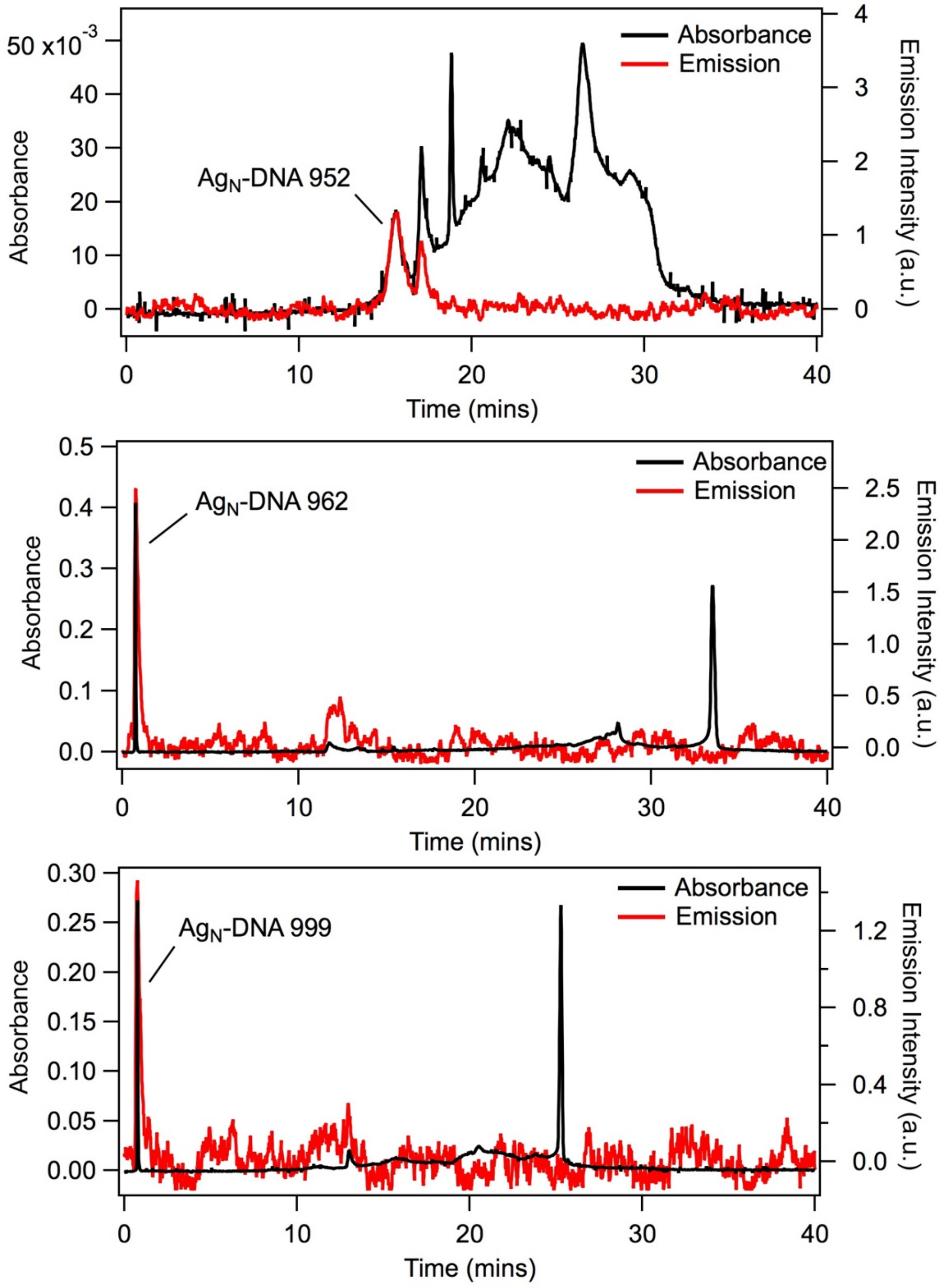

Figure S2. HPLC chromatograms of the absorbance monitored at 260 nm (black) and NIR emission (red) for Ag$_N$-DNA 952 (top), Ag$_N$-DNA 962 (middle) and Ag$_N$-DNA 999 (bottom). Fluorescence was excited at 270 nm, and measured using an 800 nm longpass filter into a broadband NIR InGaAs detector. The effective detection band for the emission chromatogram is 800 nm-1400 nm. The elution times for the high Stokes shift (SS) emitters Ag$_N$-DNA 962 (SS = 275 nm) and Ag$_N$-DNA 999 (SS = 314 nm) are much shorter than for Ag$_N$-DNA 952 (SS = 99 nm). Apparently the high Stokes shift emitters are differently structured.

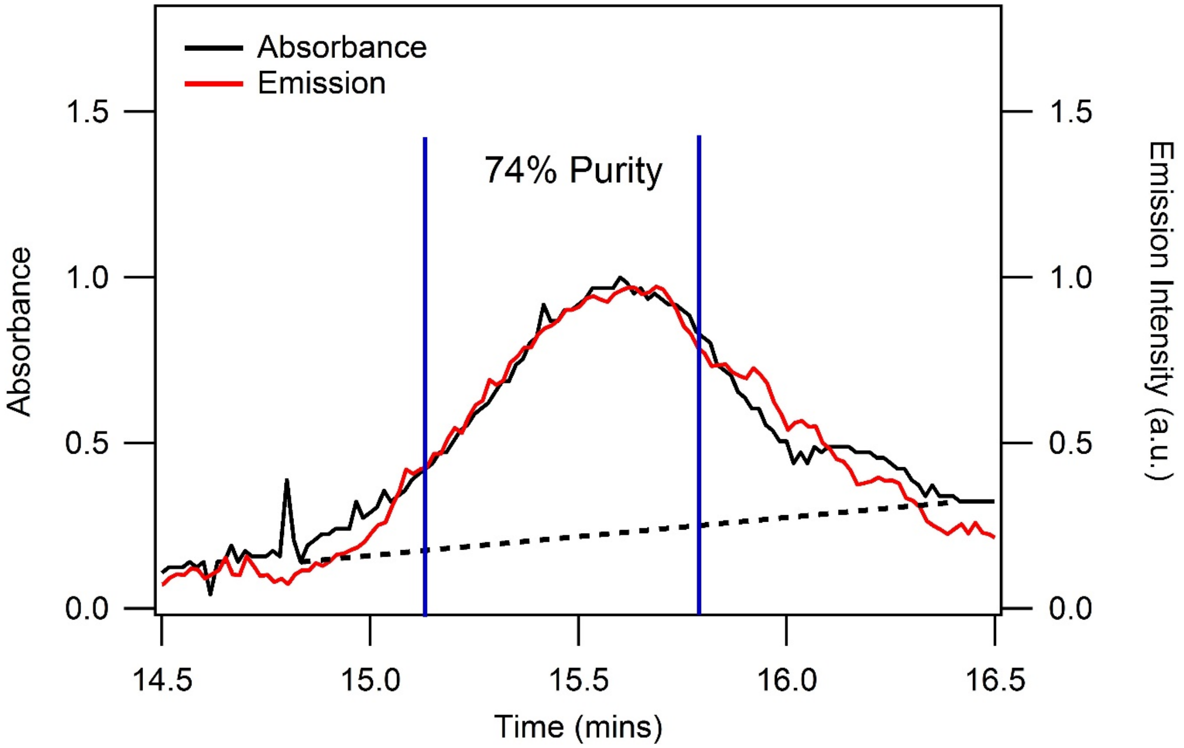

Figure S3. Purity estimate for the HPLC-purified aliquot of Ag_N-DNA 953 that was used for mass spectral analysis. Absorbance monitored at 260 nm (black curve), emission excited at 270 nm (red curve), time span of aliquot collection (blue bars) and estimated absorbance background (black dashed line). Comparison of emission spectrum to absorbance spectrum and absorbance background yields a purity estimate of 74%.

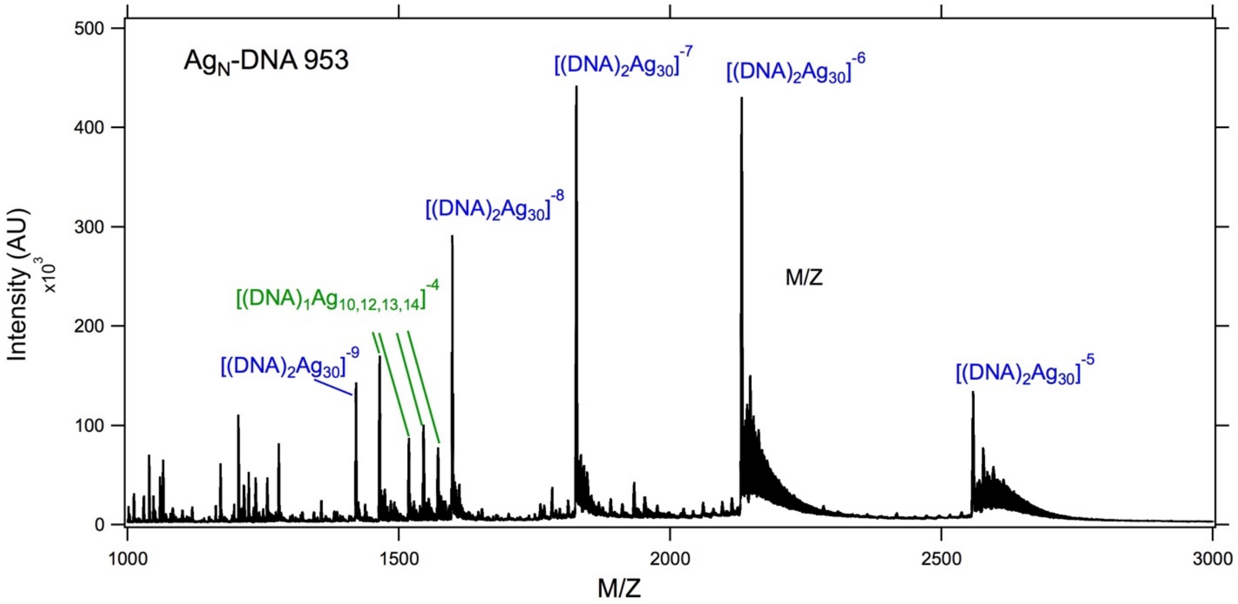

Figure S4. ESI-MS of the HPLC-purified aliquot of Ag_N-DNA 953. This is an expanded scale version of Fig. 3 in the main text, with additional labeling of products.

As discussed in the main text and the caption of Fig. S3, the fluorescent silver cluster is the major (74%) product in the HPLC-purified aliquot of Ag_N-DNA 953 analyzed by ESI-MS. Thus we can confidently identify the composition of the fluorescent silver cluster as the major, and dominant, product in ESI-MS (blue labels). This product, $(CGCCCCCACGCGCGGC)_2Ag_{30}$, contains two DNA strands held together by 30 silver atoms.

Each main $(CGCCCCCACGCGCGGC)_2Ag_{30}$ peak (labeled in blue) has an envelope of salt adduct peaks at higher M/Z. The minor products in ESI-MS, labelled in green for the Z = -4 charge state, contain one DNA strand and 10, 12, 13 and 14 silver atoms. (The same minor product peaks repeat at lower M/Z for higher Z charge states).

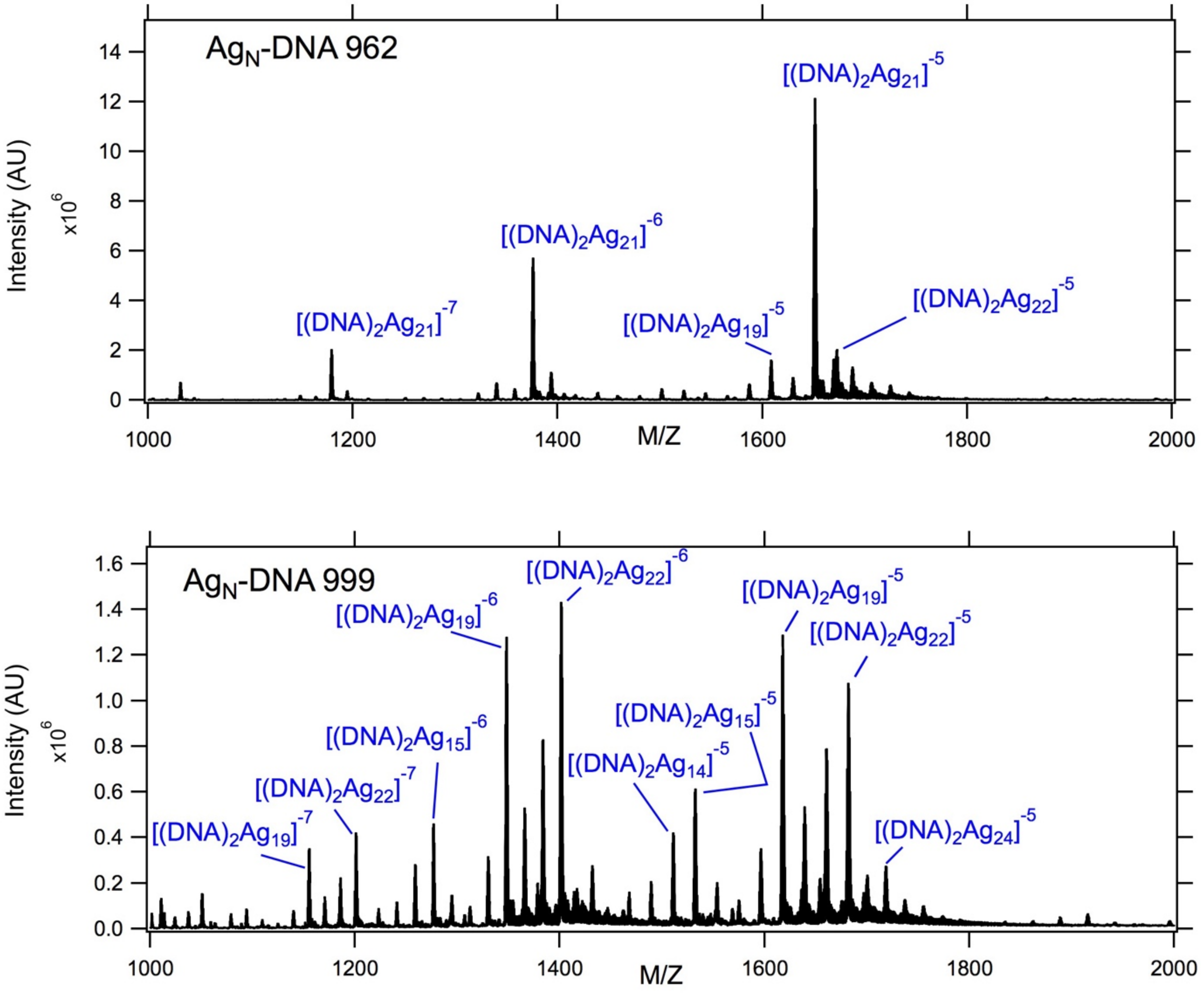

Figure S5. ESI-MS of the HPLC-purified aliquots of Ag$_N$-DNA 962 and Ag$_N$-DNA 999.

For Ag$_N$-DNA 962, all detected products contain two DNA strands and 18-26 silver atoms, with 21 silver atoms in the most abundant product (top panel).

For Ag$_N$-DNA 999, all detected products contain two DNA strands (bottom panel). Products with 14, 15 and 18-22 silver atoms are present in roughly comparable abundances and products with 12, 13 and 24-26 silver atoms are detectable.

As stated in the main text, the short elution times of the NIR-fluorescent products (Fig. S2), with instrument-limited chromatogram peak widths, did not permit estimates of purity. Thus it is unknown whether the fluorescent silver cluster is the dominant product in the aliquot captured for ESI-MS and it is not possible to assign a composition for Ag$_N$-DNA 962 or Ag$_N$-DNA 999.

Table S1. List of template sequences, intensity-weighted average emission wavelengths <λ> and integrated emission intensities for the templates which produced fluorescence with <λ> ≥ 750 nm. Values of <λ> were calculated from the spectral data for the *unpurified* samples in the three microplates studied, using emission data collected by a NIR fluorescence well plate reader (see main text). Spectral shifts of these well plate samples relative to HPLC purified material arise from the purification process, which isolates column-stable Ag_N-DNA products with elution times corresponding to specific conformations. *Red and blue entries*: Synthesis was repeated at a larger scale for HPLC purification. *Blue entries*: Spectra for the HPLC-purified samples are shown in Figure 2 of the main text.

Sequence	<λ> (nm)	Intensity (AU)	Sequence	<λ> (nm)	Intensity (AU)
TCC GGG TCG C	750.2	0.79	CCG GGG CAT A	780.4	0.02
GTG ATC CCG C	750.4	0.05	TGG GGT TCC G	780.7	0.01
AGC CGG GGC G	750.4	0.01	GCC GGG GCG C	781.4	0.08
CCG GGC CCG T	750.5	0.20	CCC ACC CAC CCG CCC A	781.4	1.64
CTC CCC GGG G	750.7	0.67	CCC CCC CCC A	781.9	1.17
GCG CGG GGG C	750.8	0.17	CCC GGG GGT C	781.9	0.32
AGG CCG GGG C	751.0	0.02	TCA GAT ATG C	783.8	0.02
CGC CCC ACG CCC	751.5	0.04	GAC GAC GGA T	783.9	2.28
CCC GGA GAA G	751.6	1.78	ACC GAC CCC C	784.0	1.90
ATC CGG GTG C	752.0	0.02	GGC GCG GCG C	785.1	0.06
CCC CGG TGA T	752.1	0.29	ATC TCC GGG G	785.6	0.04
GCC CCC GGG G	752.7	0.20	CCC GGG CGG G	785.8	0.19
TTG GCT CCC G	753.0	0.21	CGA CCC CGG A	785.9	0.49
ATC GCA GCG G	753.1	0.51	CCC CCG GGC G	788.8	1.35
GGG ATC CCC G	753.1	0.82	GCG CGC GGA A	789.3	0.10
CCC GGG CCA G	753.5	0.09	CCG GTC CGG C	789.3	0.71
CCT GGG GAA A	754.6	0.63	CCA TTC CAC C	789.9	0.46
GAC CCC CGG G	754.8	0.72	GTA TCC TCG C	790.2	0.19
CCC CGG GCA G	755.0	0.79	CCC CGG GCG C	793.3	0.98
CCG GGG GCG T	755.9	0.02	GTG GGG CGA A	793.5	0.20
CCG GGG GCC C	756.0	0.23	CCG TCC GGG G	793.8	0.26
CCA GGG GTC C	756.2	0.21	CGG GCC CGG A	795.3	0.05
CCC TGG GGC G	756.8	0.24	AGA CAA GTA C	796.9	0.76
CCC CGG CCG G	756.8	0.31	GGG GGC GAA C	797.0	0.04
GTC CGG GAG G	756.9	0.02	TCG ATC CCG C	797.1	1.94
GGG GCC GGG A	757.1	0.06	GCC CGG GCC C	798.0	0.01
CCC AAC CCG A	757.7	1.58	GTG GGG AAC G	798.1	0.23
GCG CCG GGG C	757.9	0.03	TTC CAG GGC G	798.1	0.52
GCC GGG GCA A	758.1	0.03	GAG GGG TAG C	799.1	0.06
CCT CCC GGG A	758.8	2.06	GGG GGC GCG C	800.6	0.15
CGC GGG GGC G	759.1	0.05	GTC CCC GGA C	800.8	0.19
ACG CGG GCG C	759.9	0.15	CCG GCC GGG C	801.0	0.04
GGC CGG CGC G	760.7	0.06	GGC CGG GAA C	803.3	0.01
AAT CTG TCC C	760.8	0.95	GAC GAG GCA A	804.2	0.15
CTG CCG GGC T	760.9	0.09	GGG GCG GGG A	804.4	0.12
GTA GTC CCT A	760.9	1.87	GGG GAA CAA A	807.5	0.65
CAG TCC GGG G	761.1	0.37	GGG GCG CGG C	810.8	0.08
CCC CGG GGC C	761.1	0.42	GCC TGG GCG C	811.4	0.71

ATC CGG GGC G	761.1	0.01	GGG GAA TAC A	812.1	0.14
ACC CCC GGG G	762.2	0.27	GGG CGA CAC CCC	822.4	0.04
GGG GAT GCC C	762.3	0.13	GGG GGG ACC C	824.7	0.38
CCG GAA TCC G	762.6	1.79	GGC GCG GAC C	825.9	0.87
ATC CCG AGC G	762.7	0.41	GGG GGT TAA A	826.5	0.01
AAT CCC CCC A	763.4	1.01	GGG GCC AAC G	826.9	0.01
TTC CCA CCA A	763.4	1.12	GGG CCC AAA C	827.9	0.74
GCC GGG AGC G	763.6	0.04	CGT TCC GGA C	828.4	0.15
GCC CCC ACG CCC	763.7	0.03	TGT AGT CCT T	836.4	0.01
GCG CGG GCC G	763.9	0.28	GCG AGA ATT G	838.1	0.10
CCT GGA GGG G	765.0	0.04	TTG GGC GCG G	840.5	0.07
CGG GCC GGG A	765.0	0.05	CGA ACC GGG C	842.0	1.47
GTC CCG GGC G	765.1	0.06	GGG GGT ATG C	852.2	0.01
CCG GGC TCC C	765.3	1.03	AGT CAC GAC A	854.6	0.81
CCC GGG GGG A	765.4	1.07	ACA ACT AAG T	854.9	0.03
CCC CGG GCC G	765.5	0.46	TGG AAC TCG T	856.4	0.05
GCC GGG GGA C	766.9	0.09	GCG GGG GCG C	857.1	0.01
CCA CGG GCA A	767.3	0.41	CGT TCC GGG G	858.3	0.02
GGG GTC CGA C	767.4	0.12	GAC ACG GAC C	861.0	1.61
CCC GGG GTT C	768.1	1.07	ATC TCC ACA G	861.1	0.09
CCC CCT GGA C	768.6	0.53	TCA CGA GAA C	861.3	0.04
GGG CGC GGG C	768.7	0.04	CGG GGG GGT C	864.7	0.02
CCG TCC CGC C	768.8	0.59	GGG CCG GAC G	867.0	0.50
CCT TGG GCG C	768.9	0.63	CCG GGC GGA C	871.4	0.47
TCC GAC CCC C	769.2	1.22	GGA CGC GGC CAT	873.5	0.12
ACC CCG GGG G	769.3	0.44	GTC CTG GGC G	887.6	0.09
GGG GTA ACC C	769.3	0.38	GGG GCT GCC G	888.5	0.06
TCC GGG ATA G	770.1	0.02	GTA GAA CGT T	889.2	0.49
CAC CTA GCG A	770.7	1.89	GAA CCC GGG C	890.5	0.75
GGG AAT CCA C	771.0	0.02	ATT CTT CTT G	891.1	0.02
ATC CCC CAA A	771.1	0.18	GTT GCC GGA C	891.2	0.10
CCG GGG GAC C	771.1	0.35	TCC CAA TAC T	892.2	0.07
AAT CCC CCA A	771.8	0.05	GTC CGG GAA T	901.9	0.02
GAT CCC GGA C	771.9	0.06	ATT CAG CTT C	906.0	0.05
CCC CCC CCA T	772.2	1.12	CCG GGC CGG A	907.7	0.29
CGG CCG GGA G	773.4	0.04	CGG ACC CGG G	913.4	0.10
GGG CGC GCG G	774.5	0.19	GGG GGG AAC C	918.0	0.09
CTG GTC CCG G	774.7	0.04	CGA ACC CGG A	921.9	0.52
GGG TGC GGA G	776.7	0.05	ACA CGA ACC G	942.2	0.93
CCG GGA TCG A	777.9	0.36	CCG GTC CCG A	942.4	0.02
CGG GGC GCG C	778.8	0.11	AGG TTC CCG G	944.3	0.02
GGG TGG TCC C	779.1	0.12	GGG GGA AGC C	956.4	0.02
CCG CGG GGT A	779.1	0.33	GGG CGA AGT A	956.8	0.08
CAG GGC CGG A	779.3	0.33	GAA CTA AAT G	959.7	0.04
CCC CGG GGG G	780.0	0.56	CCT GGC CGG A	962.5	0.51
CCG GGG GCA A	780.0	0.55	CGC CCC CAC GCG CGG C	972.3	0.69